



Article

A Polynomial Model for Estimation of Ex-Vivo HIFU Thermal Lesion Dynamics Based on Pressure Amplitude and Sonication Time

Francesca Parrotta ^{1,2,*} , Selene Tognarelli ^{1,2} and Arianna Menciassi ^{1,2} ¹ The BioRobotics Institute, Scuola Superiore Sant'Anna, 56127 Pisa, Italy² The Department of Excellence in Robotics and AI, Scuola Superiore Sant'Anna, 56127 Pisa, Italy

* Correspondence: francesca.parrotta@santannapisa.it

Featured Application

This work supports HIFU thermal treatment planning by providing a fast and intuitive tool for treatment parameter selection. Based on a polynomial model derived from validated numerical simulations, a desktop application is developed to compute source pressure amplitude and sonication time depending on the desired lesion dimensions. This approach enables the configuration of treatments in a reproducible way, supporting the planning of standardized therapeutic ultrasound procedures.

Abstract

High-intensity focused ultrasound (HIFU) thermal therapy exploits concentrated acoustic energy to ablate pathological tissues with millimetric precision deep in the body. Accurate prediction of thermal effects is essential for tuning the treatment shooting parameters—such as source pressure amplitude and sonication time—as well as for maximizing efficacy and preserving surrounding healthy tissue. This study presents a computational model developed in COMSOL Multiphysics to simulate the physics of HIFU thermal phenomena, accounting for acoustic propagation and heat diffusion in biological tissues. The model was validated through experimental tests on ex vivo chicken breast tissue within a robotic ultrasound-guided HIFU (USgHIFU) platform, with lesion dimensions serving as the primary metric for validation. Building upon the validated simulation, we define a polynomial-based model that analytically predicts lesion dimensions based on the input shooting parameters. This approach significantly reduces the COMSOL computational cost and execution time, making it well-suited for integration into a real-time treatment planning workflow for clinical use. A desktop application implementing the inverse formulation of the polynomial model was developed, allowing shooting parameters to be computed from target lesion dimensions through a simple and intuitive interface. By enabling a rapid estimation of lesion size, this solution supports a more standardized strategy for non-invasive oncological therapies.



Academic Editor: Georges Wagnieres

Received: 5 January 2026

Revised: 8 February 2026

Accepted: 11 February 2026

Published: 12 February 2026

Copyright: © 2026 by the authors.

Licensee MDPI, Basel, Switzerland.

This article is an open access article distributed under the terms and conditions of the [Creative Commons Attribution \(CC BY\)](https://creativecommons.org/licenses/by/4.0/) license.

Keywords: HIFU surgery; thermal ablation; predictive model

1. Introduction

Ultrasound (US) is a form of mechanical energy that is transmitted through and into biological tissues as an acoustic pressure wave at frequencies above the limit of human hearing, and it is widely used in medicine as a diagnostic, therapeutic, and surgical tool.

In high-intensity focused ultrasound (HIFU) medical treatment, US energy emitted by a transducer is focused into a small volume to heat and destroy the targeted tissue, while ideally not damaging tissues outside the focal region [1]. The use of US as a surgical instrument involves high levels of intensity (up to 300 W/cm^2), and sharp bursts of energy can be used to fragment calculi or to ablate tissues such as those affected by cancer [2]. Main US parameters, such as wave intensity and sonication time, should be adjusted according to the desired type of effect on tissues and the available hardware [3]. We refer to these indicators as shooting parameters.

Based on the above premise, the guiding principle of HIFU is that an ultrasonic beam should be able to rapidly destroy a sharply defined region of tissue [4,5]. Furthermore, recent developments in medical robotics showed that integrating the therapeutic transducer within a robotic platform can enable precise and automatic HIFU beam control [6,7], with the ultimate goal of further increasing the accuracy of these procedures and reducing the therapy time. These applications depend on the direct interaction of the ultrasound field with the tissue and can be used to create either a low-level thermal rise, in general up to around 45°C (local hyperthermia), or a short, highly localized temperature rise up to $60\text{--}65^\circ\text{C}$ (thermal ablation). Specifically, it is known that 60°C is the temperature threshold that leads to complete cell killing [8]. Ultrasound-induced temperature rise is dependent on several factors, including tissue properties (e.g., absorption coefficient, density, perfusion rate, etc.) as well as ultrasound exposure parameters (e.g., frequency, pressure amplitude, pulse duration, pulse repetition frequency, etc.) [9,10]. The temperature elevation in a region subjected to an acoustic disturbance is the direct result of acoustic power absorption in the region of interest, as the absorption of ultrasound results in the conversion of ultrasonic energy to heat [11,12]. This study is dedicated to the analysis of thermal ablation phenomena.

A key point related to the thermal effect is to precisely determine the extent of the lesioned tissue, which can enable the planning of effective sonication of cancer areas. HIFU has demonstrated efficacy in non-invasive tumor ablation, but several limitations affect its application, including the overheating of surrounding tissues and challenges in maintaining precise beam focusing at the intended treatment area [13]. These limitations arise from both the physical properties of ultrasound propagation and the anatomical and physiological characteristics of tissues. Moreover, the choice of shooting parameters currently depends only on the operator's experience, pointing out the absence of a standardized and objective procedure.

For this reason, finite element methods (FEMs) have been widely used for HIFU simulations. Several numerical models have been proposed to simulate the propagation of focused ultrasound waves into tissues, highlighting the importance of treatment planning and the optimization of therapeutic outcomes. However, currently there is no gold standard for computational simulations concerning HIFU treatment. Most work in the state of the art uses k-Wave toolbox (MATLAB R2024b, The MathWorks Inc., Natick, MA, USA) as the software interface [14–16], and many scientific papers [17–19] present an experimental validation of the mathematical model, but they focus on acoustic pressure and temperature mapping without assessing the formation of ablated tissue, which is the most critical parameter when planning a full ablation procedure.

An alternative environment for studying complex phenomena, such as those involved in HIFU, is COMSOL Multiphysics 6.2 (COMSOL Multiphysics, COMSOL AB, Stockholm, Sweden), owing to its purpose-built architecture for Multiphysics simulations and its intuitive user interface. Montienthong et al. [20] developed an FEM-based computational model using COMSOL to simulate HIFU treatment for breast cancer by estimating the thermal distribution and tissue deformation during ablation. The study lacks experimental

validation on phantoms or ex vivo tissues, and it exhibits the same previously discussed limitations concerning lesion formation.

Conducting experimental tests in this field is complex and non-trivial because this usually involves ex vivo tissues and can therefore cause resource consumption and expensive solutions, in addition to the fact that thermal data on biological tissues remain limited in the literature because of the high variability among biological samples [21]. Referring to tissue properties, the absorption coefficient (α) plays a pivotal role, as it determines how energy is absorbed by the tissue and converted into heat, directly affecting lesion formation and treatment precision.

To fulfil the abovementioned objectives, and in particular the need for a standardized method to establish lesion size in HIFU therapy, we propose a polynomial approach that enables the definition of lesion dimensions based on acoustic and thermal analyses, given source pressure amplitude and sonication time as the input parameters. The approach is tissue-specific, as it depends on the absorption coefficient, but it becomes general once the specific absorption coefficients are known for the selected tissues. This polynomial equation is derived from a COMSOL Multiphysics 6.2 numerical model and serves as its surrogate, offering significant advantages in terms of complexity and computational cost, with execution times reduced to just a few seconds.

The structure of the present article is as follows. Section 2 presents the materials and methods, including the COMSOL Multiphysics 6.2 computational model, the experimental activity conducted on ex vivo chicken breast tissue, the methodology used to derive the polynomial relationship between treatment parameters and lesion dimensions, and the development of a desktop application implementing the inverse polynomial model as a clinician-oriented planning tool. Section 3 reports the corresponding results, including a simulation validation against experimental data, the final polynomial formulation, and the first implementation of the desktop application. The discussion and future perspectives are presented in Section 4.

2. Materials and Methods

2.1. Computational Model

Propagation of HIFU through a tissue was studied using a COMSOL Multiphysics 6.2 computational model, as the first step of the workflow in this study, shown in block (a) of Figure 1.

The geometry of the model was 2D-axisymmetric, as this is an intrinsic feature of the HIFU beam [22], and it was represented in cross-section, as shown in Figure 2. A ring-shaped focused ultrasound transducer with a concave lens was used to emit the signal reaching the highest intensity within a focal zone, for consistency with the experimental conditions, which will be further explored later in the article. The simulated geometry included 105 mm of water above 30 mm of tissue. Water is essential for acoustic coupling, and the lesion was expected to form at the center of the tissue, corresponding to the focal length ($F = 120$ mm) of the focused transducer. To define an open boundary condition, two absorbing layers (one in the horizontal direction and one in the vertical direction) were added to the geometry as a perfectly matched layer (PML) to slow down wave propagation and prevent artificial reflections of acoustic waves at the domain edges.

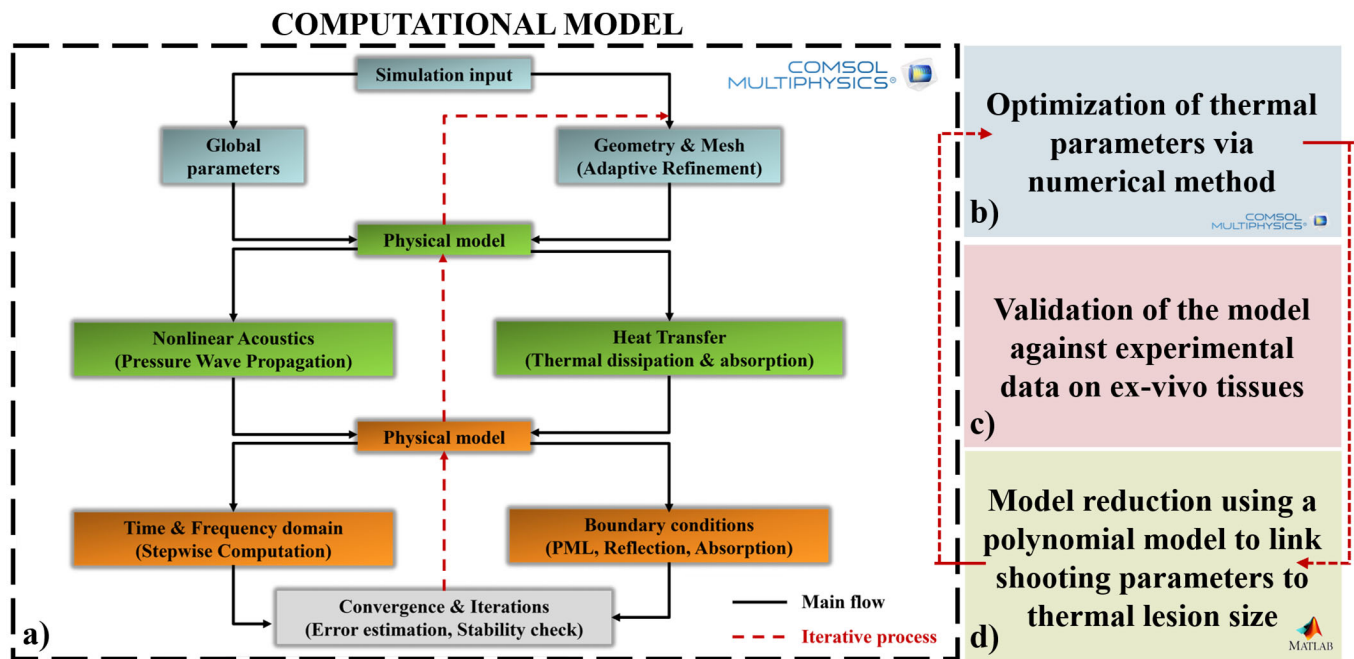


Figure 1. Block diagram of the proposed workflow. (a) The HIFU thermal lesion mechanism is modeled using a multiphysics computational approach, where open boundary conditions are implemented through perfectly matched layers (PML) to minimize reflections at the edges of the computational domain. (b) A thermal parameter optimization step is introduced. (c) Numerical results are validated against experimental measurements. (d) The validated model is reduced by deriving a polynomial function that describes the thermal lesion dimensions as a function of the HIFU shooting parameters.

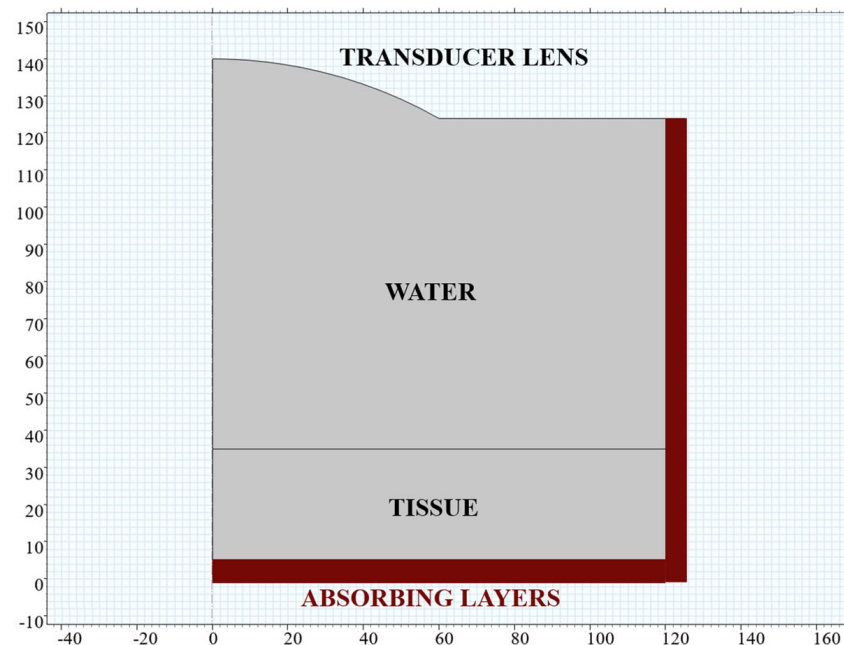


Figure 2. Geometry of the computational model. A focused ultrasound transducer equipped with a concave lens emits the acoustic signal through 105 mm of water, used for acoustic coupling, and into 30 mm of tissue. The thermal lesion is expected to form at the focal length of the transducer ($F = 120$ mm). Absorbing layers are added to the geometry as perfectly matched layers (PML) to define the boundary conditions and minimize wave reflections.

The US wave characteristics were determined using our experimental hardware, whereas reference was made to the COMSOL Application Library for the computational model parameters [23]. The therapeutic HIFU transducer had a central frequency of 1.2 MHz and focal length of 120 mm (Imasonic, Voray-sur-l'Ognon, France), and it was driven by a 16-channel high power signal generator (Image Guided Therapy, Pessac, France). Each channel could reach up to 20 W, thus generating a maximum power of 320 W, which resulted in a maximum signal amplitude of $P0_max = 304.6$ kPa, according to the relationship that links power [W] to source pressure amplitude [Pa] [22]:

$$P0 = \sqrt{\frac{2\rho cP}{A}},$$

where ρ and c are the density and the speed of sound in water, respectively; P is the maximum power [W] that can be emitted by the wave generator; and A is the area of the therapeutic transducer. It had the shape of a circular ring with an outer diameter of 120 mm and an inner diameter of 35 mm. All simulation input parameters are listed in Table 1.

The COMSOL Multiphysics 6.2 model was multiphysics in nature: propagation of the HIFU signal exploited the Pressure Acoustics, Frequency domain physics interface, while thermal phenomena resulting from the propagation of the US waves in tissues were investigated through the Heat Transfer interface. The interfaces solved the system of nonlinear acoustic equations in the form of a hyperbolic conservation law [24], using the discontinuous Galerkin finite element method [25] and an explicit time integration scheme. To consider the fact that a 90% duty cycle is typically applied in UsgHIFU applications [7] to allow correct visualization of the guiding ultrasound imaging, the Events interface was added to the model. The numerical study consisted of two sequential steps: first, the acoustic pressure was analyzed in the frequency domain, and this node then served as the input for a time-domain thermal analysis, which also accounted for the considered duty cycle. The considered time interval was 10 s, with a time step of 1 s.

The thermal model—at this stage—was formulated to account for heat transfer governed by thermal conduction only, consistent with the ex vivo validation conditions adopted in this study, where blood perfusion effects are inherently absent [26]. The initial tissue temperature was assumed to be 20 °C (room temperature), in accordance with the experimental conditions.

To solve the geometry (Figure 2) in accordance with the implemented physics, the mesh had to be fine enough to resolve the frequency content of the signal. A mesh convergence analysis was conducted to verify mesh independence, and a discretization corresponding to six finite elements per wavelength was selected for all simulations. The primary objective of this model was to study tissue thermal damage, particularly as a function of the combination of source pressure amplitude and sonication time. Therefore, in addition to the temporal analysis, a parametric study on pressure was included that considered 7 scale factors, ranging from 0.35 to 0.65 with a step size of 0.05. The scale factors indicated the percentage of the maximum pressure value achievable with our power signal generator (304.6 kPa). Together with the sonication time, the scale factors represented a critical factor in defining the shooting parameters, as both directly influence the delivered acoustic energy.

To evaluate lesion dimensions, reference was made to the classical ellipsoidal shape of the thermal lesion induced by HIFU treatment [12], with D1 defined as the maximum vertical dimension (major axis of the ellipse) and D2 defined as the horizontal one (minor axis of the ellipse). The condition to be satisfied for classifying a tissue region as a lesion was that the local temperature must exceed 60 °C [8]. To define the lesion dimensions as simulation outputs, we specified two variables, c1 and c2, for D1 and D2, respectively. Specifically, the maximum of the general projection for variables c1 and c2 over the projection domain

was evaluated. The general projection operator computed a spatial mapping of a field variable—temperature in our case—from one geometric entity to another, by integrating the field over the source domain and associating the resulting value with points in the target domain. This involved a weighted integral of the field, allowing complex coupling between different physical domains or geometric components in the model. Based on this, a study of the lesion shape as a function of source pressure amplitude and sonication time was conducted, as lesion assessment represents a fundamental step in preoperative planning [27].

Given the simulation validation and the limited availability of thermal data reported in the literature [21], the tissue absorption coefficient (α_{tissue}) was optimized through numerical methods in COMSOL Multiphysics 6.2 (Figure 1b). This optimization phase was specific for the tissue used in the experimental conditions under investigation, i.e., chicken breast in our case. A specific shooting parameters combination was selected, i.e., the experimental conditions Scale Factor = 60% and Sonication Time = 5 s. This choice was motivated by the fact that it was the most frequently adopted setting in the literature [7]. To this end, parametric studies on α_{tissue} were carried out, varying it with respect to the default COMSOL Multiphysics 6.2 value ($\alpha_{tissue} = 8.55$ [1/m], Table 1).

Table 1. Input parameters of the COMSOL Multiphysics 6.2 simulation. Parameters characterizing the ultrasound (US) wave, which are specific to the experimental hardware, are listed above the bold line. The remaining parameters, required for solving the computational model, are taken from the COMSOL Application Library (“High-Intensity Focused Ultrasound (HIFU) Propagation Through a Tissue Phantom”, n.d.) and are reported below the bold line.

Parameters	Expression	Description
P0_max	304.6 [kPa]	Source pressure amplitude
ScaleFactor	0.35–0.65	Pressure amplitude scaling factor, ranging from 0.35 to 0.65 (parametric study)
P0	ScaleFactor · P0_max	Scaled source pressure amplitude
f0	1.2 [MHz]	Source frequency
omega0	$2 \cdot \pi \cdot f0$	Source angular frequency
T0	$1/f0$	Source period
F	120 [mm]	Focal length
r_source	120 [mm]	External diameter of the transducer
r_hole	35 [mm]	Internal diameter of the transducer
th_abs	5 [mm]	Thickness of the absorbing layer
th_tissue	30 [mm]	Height of the tissue layer
th_water	105 [mm]	Height of the water layer
alpha_water	0.025 [1/m]	Absorption coefficient of water at ~1 MHz
alpha_tissue	8.55 [1/m]	Absorption coefficient of tissue at ~1 MHz
c_water	1484 [m/s]	Speed of sound in water
c_tissue	1568 [m/s]	Speed of sound in tissue
rho_water	1000 [kg/m ³]	Density of water
rho_tissue	1044 [kg/m ³]	Density of tissue
BA_water	5.2	Parameter of nonlinearity of water
BA_tissue	7.4	Parameter of nonlinearity of tissue
delta_water	$2 \cdot \alpha_{water} \cdot c_{water}^3 / \omega_{0}^2$	Sound diffusivity of water
delta_tissue	$2 \cdot \alpha_{tissue} \cdot c_{tissue}^3 / \omega_{0}^2$	Sound diffusivity of tissue

2.2. Experimental Tests for Model Validation

Experimental tests on an ex vivo chicken breast phantom were carried out to validate the computational model described in the previous paragraph, in the context of a robotic US-guided platform for HIFU (USgHIFU) surgery, as shown in Figure 3. A Doosan robotic arm (M0609, Doosan Corporation, Seoul, Republic of Korea) held a therapeutic HIFU transducer, specifically a 16-channel phased annular array transducer with a cen-

tral frequency of 1.2 MHz, diameter of 120 mm, and focal length of 120 mm (Imasonic, Voray-sur-l'Ognon, France). The HIFU transducer was connected to a high-power signal generator, which was capable of delivering up to 320 W of power. A robot–phantom base frame calibration was performed to control the exact position of the transducer and thus of the focal point. The therapeutic transducer was integrated with a confocal 2D phased US probe (P5-1S15A-6, Telemed, Vilnius, Lithuania) for target visualization. The images provided by the US probe guaranteed monitoring of HIFU transducer positioning and treatment. US wave propagation was optimized by fully surrounding the tissue with water and integrating an acoustic absorber into the support structure. A water tank filled with deionized and degassed water (dd-H₂O) was employed, and a custom-made support structure securely held the tissues, preventing any relative movement.

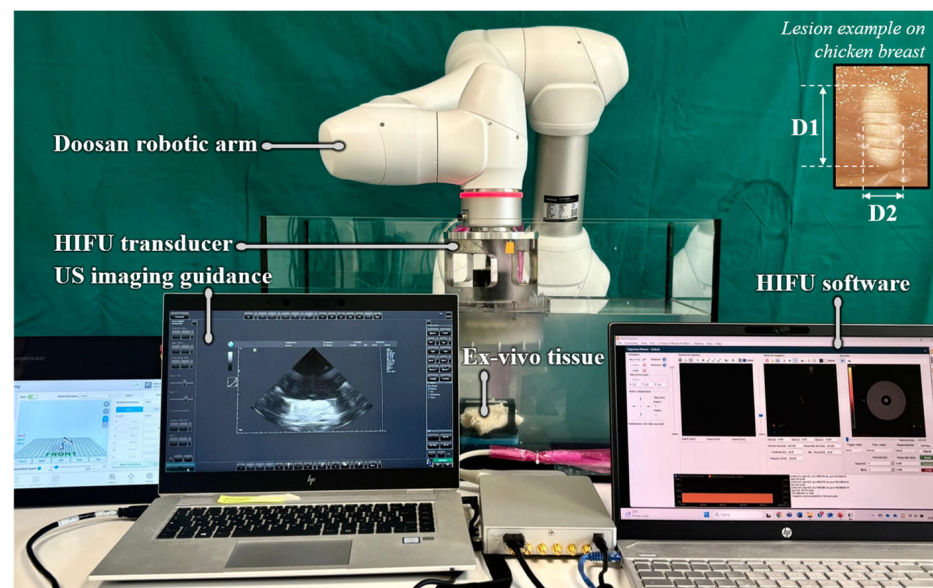


Figure 3. Robotic USgHIFU experimental set-up. A focused ultrasound transducer is held in place by a customized holder mounted on a Doosan robotic arm. The sonication procedure is performed on an ex vivo chicken breast phantom positioned at the center of a water tank filled with deionized and degassed water (dd-H₂O) and is guided by a TELEMED phased-array ultrasound probe. On the right, an example of a thermal lesion obtained in ex vivo chicken breast tissue is shown, where D1 denotes the major axis and D2 denotes the minor axis of the elliptical lesion.

Six experimental conditions were tested, performing 6 repetitions for each condition. The following Scale Factor [%]—Time [s] combinations were investigated: (i) 55%—5 s; (ii) 55%—10 s; (iii) 60%—5 s; (iv) 60%—10 s; (v) 65%—5 s; and (vi) 65%—10 s. The results in terms of lesion dimensions were measured after the shot using both a digital caliper and a digital microscope (HRX-01 3D, Hirox-USA, Oradell, NJ, USA), equipped with an MX-MACROZ IV lens (20× magnification). These values were then compared with the computational model results.

2.3. Predictive Polynomial Model

The objective of this section is to explore a direct correlation between the dimensions of the HIFU-induced lesion and the shooting parameters, with the aim of reducing the computational cost associated with numerical simulations. Following simulation validation in terms of lesion dimension through experimental results on ex vivo chicken breast tissue, a mathematical function $D_{1,2}(p, t)$ was investigated, considering: (i) lesion dimension ($D_{1,2}$); (ii) source pressure amplitude (p), considering different scale factors (scaled p); and (iii) sonication time (t). An interpolation surface was obtained linking these three variables (D ,

p , and t) using the `interp2` MATLAB R2024b function, notably applying the spline method, based on the data extracted from the COMSOL Multiphysics 6.2 simulation. The result of this analysis was a quadratic polynomial with two variables, for which the analytical coefficients were computed.

After determining the optimal absorption coefficient through a parametric study on α_{tissue} , the polynomial function was calculated (Figure 1d) with the new $\alpha_{\text{tissueOptimized}}$, and errors between the lesion dimensions obtained from the COMSOL Multiphysics 6.2 simulation and those predicted by the optimized analytical polynomial are evaluated. This approach aimed to develop a surrogate of the computational model while significantly reducing computational cost and time (Figure 1d), thereby enabling real-time preoperative planning of HIFU procedure.

2.4. Translation of the Polynomial Model Under Perfused Tissue Conditions

To extend the proposed framework toward conditions that are more representative of in vivo applications, the numerical model was modified to explicitly account for blood perfusion effects within the bioheat formulation [26]. In particular, the perfusion-driven heat exchange term was enabled in the bioheat equation, while maintaining the same acoustic and thermal modeling strategy adopted in the non-perfused case. The tissue absorption coefficient was set to $\alpha = 8.55$ [1/m] (tissue-related value), and the initial tissue temperature was assumed to be 37 °C, consistent with physiological conditions. This approach was intended to introduce a numerical correction that accounted for physiological effects, building upon a model previously validated under simpler and more controllable ex vivo experimental conditions.

Blood perfusion values were selected based on literature data for hepatic tissues [28], considering that liver tumors may exhibit either hypo-perfused or hyper-perfused behavior depending on tumor type and vascularization [29]. To capture a clinically meaningful and representative scenario, an average perfusion value was then adopted.

A double parametric study was performed. First, the acoustic scale factor was varied over an extended range compared to the non-perfused ex vivo case (0.35–0.65), under the assumption that higher energy deposition may be required to achieve thermal ablation in perfused tissue due to perfusion-driven heat removal. Second, simulations were carried out both with and without blood perfusion, enabling a direct and quantitative comparison between perfused and non-perfused conditions.

To establish a quantitative correspondence between perfused and non-perfused conditions, an equivalence criterion based on lesion dimensions was defined. In this analysis, the equivalence between perfused and non-perfused conditions was defined at a fixed sonication time of 10 s, which represented the maximum duration considered in the study. For each sonication time, lesion dimensions (D_1 , D_2) obtained under non-perfused conditions were taken as references. The corresponding perfused scale factor was then identified as the value producing thermally equivalent lesions by minimizing the difference between perfused and non-perfused lesion dimensions. This procedure allowed the definition of an equivalent scale factor mapping between the two regimes and the identification of the scale factor range required under perfused conditions to reproduce lesion sizes obtained in the non-perfused case.

2.5. HIFU Treatment Planning Tool

The polynomial model was further exploited to develop a clinical tool aimed at supporting real-time HIFU thermal treatment planning. A dedicated desktop application was implemented using MATLAB App Designer, allowing clinicians to directly prescribe target lesion dimensions and automatically obtain the corresponding shooting parameters.

Unlike the forward predictive model described in the previous section, the tool relied on the inverse use of the polynomial interpolation surfaces, where the desired lesion diameters (D_1 and D_2) were provided as inputs.

To determine the treatment parameters, the problem was formulated as a constrained optimization task. An objective function was defined to quantify the absolute errors on D_1 and D_2 between the target lesion dimensions specified by the user and those predicted by the polynomial model. The optimal treatment parameters were obtained by solving the constrained nonlinear optimization problem using the MATLAB R2024b *fmincon* function. The resulting solution corresponded to the minimum of the objective function and yielded the set of shooting parameters that best reproduced the input lesion geometry within the validity domain of the model. The optimization variables were constrained to the source pressure amplitudes corresponding to the thermally dominated regime (see Section 3.3 in the Results for details) and to sonication times ranging from 0 to 10 s.

3. Results

3.1. Computational Model Results

3.1.1. Acoustic Pressure

The main result of the Pressure Acoustic, Frequency domain node from the computational model was the evaluation of the acoustic pressure distribution within the considered geometry. Different levels of source pressure were evaluated according to scale factors. Figure 4 presents the pressure maps for two different source pressure levels (corresponding to scale factor values of 0.5 and 0.6), with two time points (5 s, 10 s) shown for each case. As expected, the pressure maps show a peak at the focal point. As the acoustic pressure and sonication time increase, the treatment effect becomes more pronounced, resulting in higher acoustic pressure levels within the focal region.

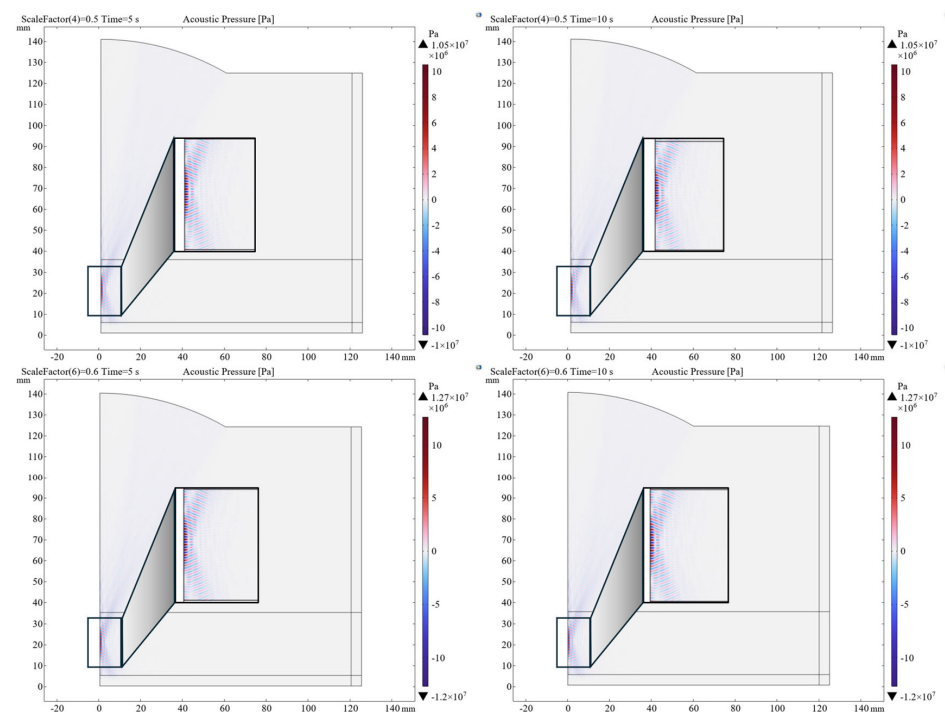


Figure 4. Acoustic pressure maps obtained for different combinations of source pressure amplitude and sonication time. The source pressure amplitude is varied using scale factors. A scale factor of 0.5 corresponds to an acoustic pressure of 152.3 kPa, while a scale factor of 0.6 corresponds to an acoustic pressure of 182.76 kPa.

3.1.2. Temperature

The main output of the Heat Transfer node in the computational model was the evaluation of thermal distribution and energy absorption phenomena in tissue following exposure to the ultrasonic wave. As observed in the pressure maps, temperature distribution also exhibits a peak at the focal point, as shown in Figure 5. As the scale factor and sonication time increase, the treatment effect becomes more pronounced, leading to higher temperature values within the focal region.

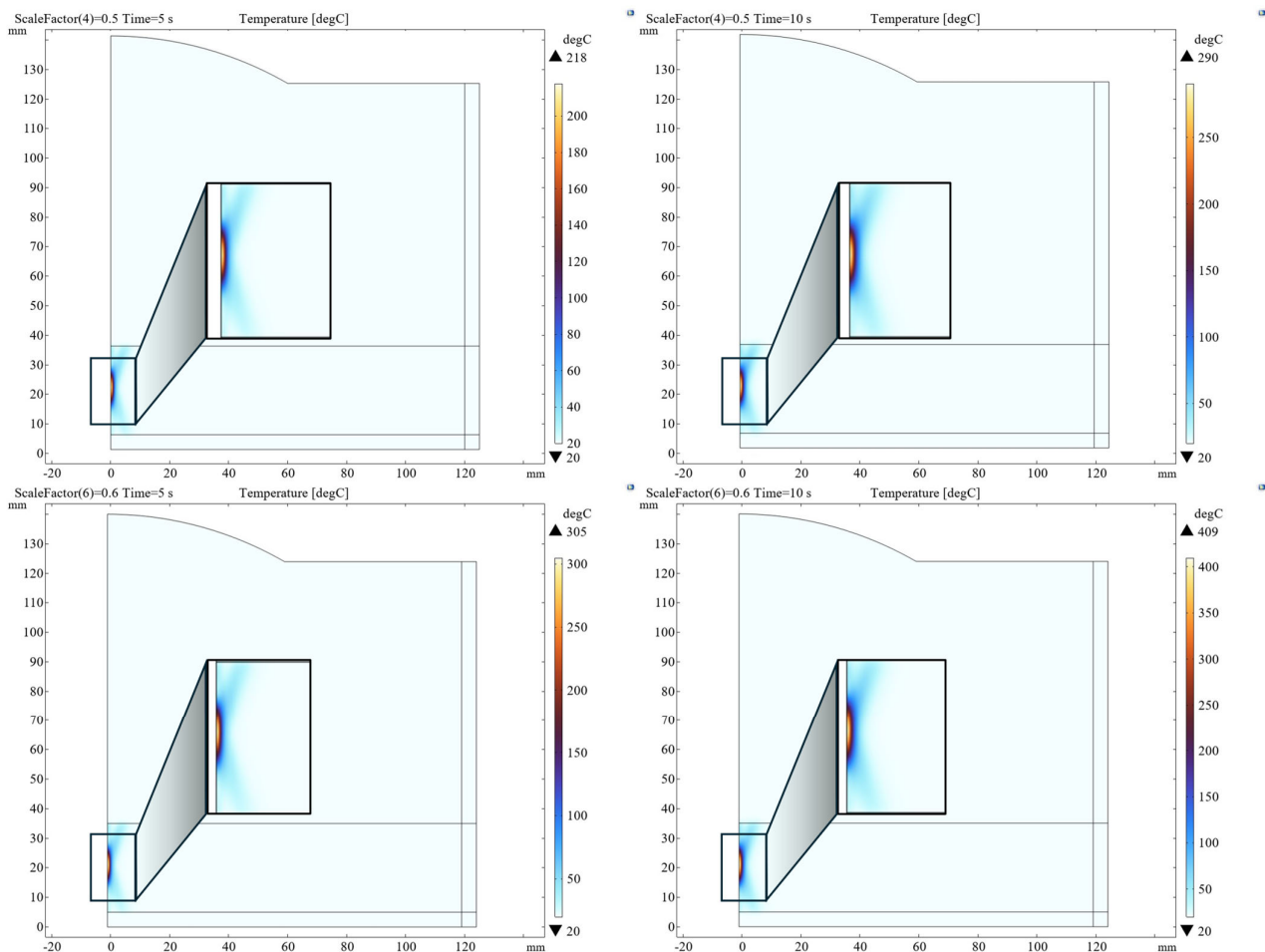


Figure 5. Temperature maps obtained for different combinations of scaled source pressure amplitude and sonication time. Different levels of source pressure are evaluated using scale factors.

3.1.3. Model Validation: Lesion Dimension

Lesion dimension was computed as the primary output of the computational model, using the general projection operator to identify the maximum spatial extent of tissue points where the local temperature exceeded 60 °C. According to the results obtained from the COMSOL Multiphysics 6.2 simulation, Figure 6 shows both lesion dimensions D1 (major axis) and D2 (minor axis). To define D1 and D2, reference was made to the axis of the ellipsoidal shape obtained for the HIFU thermal lesion, for which a representative example is reported in Figure 6 as well. Figure 7 reports the comparison between the lesion dimensions obtained experimentally and those predicted by the COMSOL Multiphysics 6.2 computational model. For the purpose of validating the computational model (Figure 1c), errors were calculated to compare the predicted lesion with the corresponding experimental measurements. The mean error in estimating D1 was 2.6 mm (20.7%), while for D2 it reached a maximum of 1.1 mm (20.3%). These values were within acceptable limits, considering

that margins up to 10 mm beyond the tumor edge are commonly regarded as safe in clinical practice [30]. The highest error in D1 estimation was observed under the 60%—5 s condition. By contrast, the error in D2 estimation exhibited a linear increase with pressure, reaching its peak under the 65%—10 s condition. This outcome was expected, as it has been experimentally observed that—with our experimental setup and following transducer characterization—cavitation effects begin to dominate beyond this power level, thus moving away from a purely thermal regime.

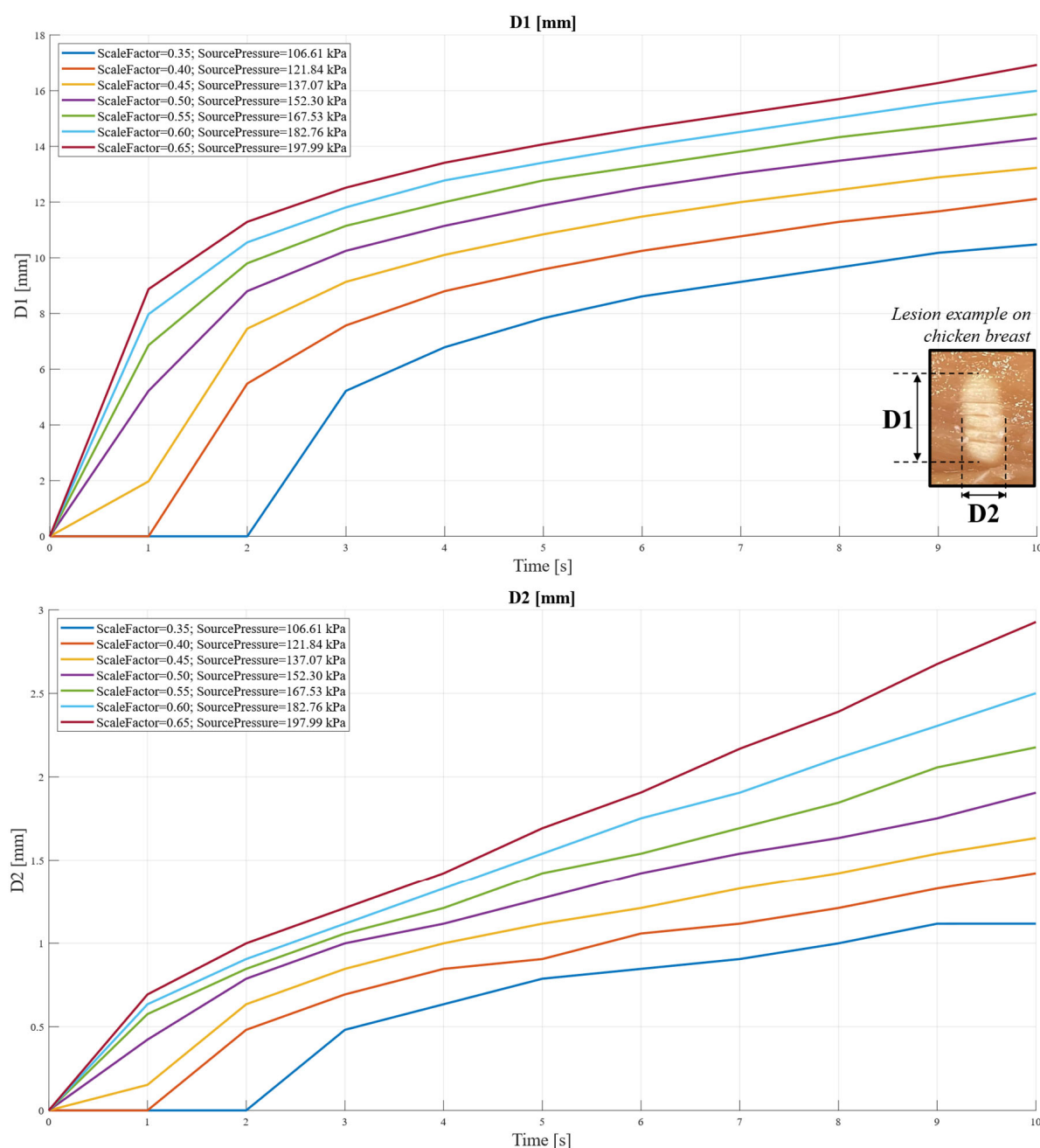


Figure 6. Lesion dimensions D1 and D2 computed in the simulation environment, representing the major and minor axes of the thermal lesion as predicted by the computational model.

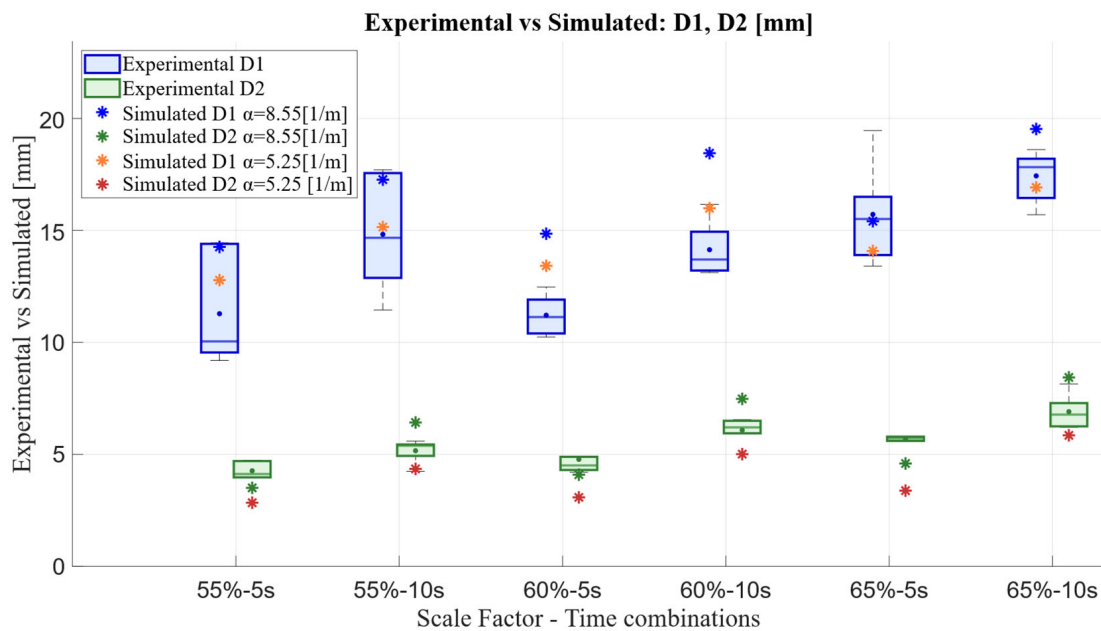


Figure 7. Comparison between lesion dimensions D1 and D2 obtained experimentally (exp) and those predicted by the computational model (simulated). Experimental variability is reported based on six repeated measurements for each Scale Factor–Sonication Time combination. The effect of tissue absorption coefficient optimization is also shown: $\alpha = 8.55$ [1/m] corresponds to the general tissue absorption coefficient from the COMSOL library, while $\alpha = 5.25$ [1/m] represents the optimized absorption coefficient for the considered ex vivo tissue.

In addition to mean error metrics, a formal Bland–Altman analysis was performed to assess the agreement between simulated and experimental lesion dimensions. This approach allowed an evaluation of systematic bias, variability, and potential pathological error patterns that cannot be captured by a mean error percentage alone. The analysis was conducted for both the non-optimized and optimized models and for both lesion dimensions (D1 and D2). For D1, the optimized model showed a reduction in bias from +2.53 mm to +0.62 mm, with a standard deviation of approximately 1.5 mm. For D2, the optimized model exhibited a reduced dispersion, with the standard deviation decreasing from approximately 1.24 mm to 0.55 mm. Importantly, no proportional bias or heteroscedasticity was detected, and the differences remained evenly distributed across the measurement range, indicating consistent model behavior across operating conditions.

Regarding thermal parameter optimization, a specific shooting parameter combination was selected, i.e., the experimental condition Scale Factor = 60% and Sonication Time = 5 s. This choice was motivated both by the fact that it exhibited the highest error in D1 estimation and because it was the most frequently adopted setting in the literature [7], as introduced in Section 2. Parametric studies for the absorption coefficient revealed distinct optimal values for D1 and D2, reflecting tissue anisotropy and the direction-dependent interaction of ultrasonic wave with biological tissues [22]. Specifically, the optimal value for D1 was $\alpha_{D1} = 4$ [1/m], while for D2 it was $\alpha_{D2} = 6.5$ [1/m], based on the proximity of the newly predicted values of D1 and D2 to an experimental dataset different from the one used for the validation of the COMSOL Multiphysics 6.2 model.

A new simulation (Figure 1b) was then performed using an average absorption coefficient, i.e., $\alpha_{\text{tissueOptimized}} = 5.25$ [1/m], and errors were re-evaluated against the experimental data reported in Figure 7. Under this optimized configuration, the mean errors were 1.3 mm (10.7%) for D1 and 1.4 mm (26.8%) for D2, with the error on D1 was reduced by approximately 50% compared to the non-optimization case, while D2 showed no significant

variation. It is worth noting that, for validation purposes, the major lesion dimension (D1) was more representative, as it was easier to detect and measure experimentally.

Therefore, in the following analyses, the simulation with $\alpha_{tissueOptimized} = 5.25$ [1/m] is considered.

3.1.4. Lesion Visualization

As previously mentioned, defining the shape of the lesion is a fundamental aspect in the study of HIFU technology. For this reason, the presented numerical model also enables a shape analysis, allowing for a visual assessment of how the treatment effect varies with changes in source pressure amplitude and sonication time. This serves as a crucial starting point for planning strategies in real tumor treatment, as it enables the estimation of how many elementary lesions are required to cover the surface of an actual tumor. This number will depend on the characteristics of each real individual lesion, which in turn are influenced by the anatomical structure being treated (e.g., proximity to a blood vessel that must be avoided).

Figure 8 presents a visualization of the shape of the elementary lesions, corresponding to two different scaled source pressure levels (corresponding to scale factor values of 0.5 and 0.6), with two distinct time points (5 s, 10 s) shown for each case. With increasing scale factor and sonication time, the treatment effect becomes more evident, leading to a progressive enlargement of the lesion.

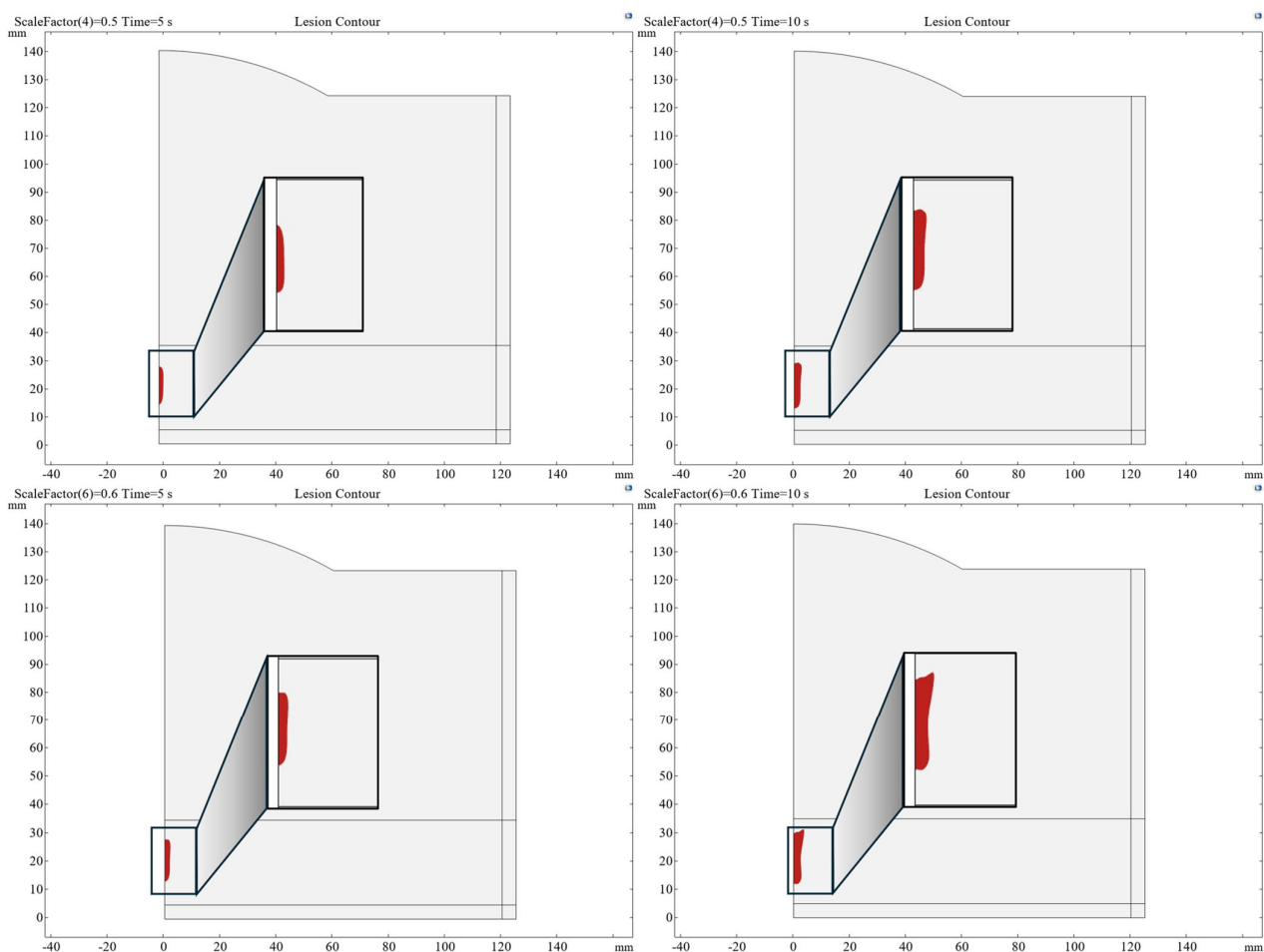


Figure 8. Visualization of lesion shape for different combinations of scaled source pressure amplitude and sonication time. The lesion size increases as the examined parameters increase.

3.2. Predictive Polynomial Function

The polynomial function was derived using the methods described in Section 2.3 and describes the surface in Figure 9. It related lesion size to a given shooting parameter combination through a second-order polynomial function with two variables, where p (source pressure amplitude) and t (sonication time) are the independent variables, while D represents the dependent variable. A single polynomial form was used for both D1 and D2, as in Equation (1), with distinct analytical coefficients required for each case, considering the analytical coefficients in Table 2.

$$D_{1,2}(p, t) = a_0 + a_1p + a_2t + a_3p^2 + a_4t^2 + a_5pt \quad (1)$$

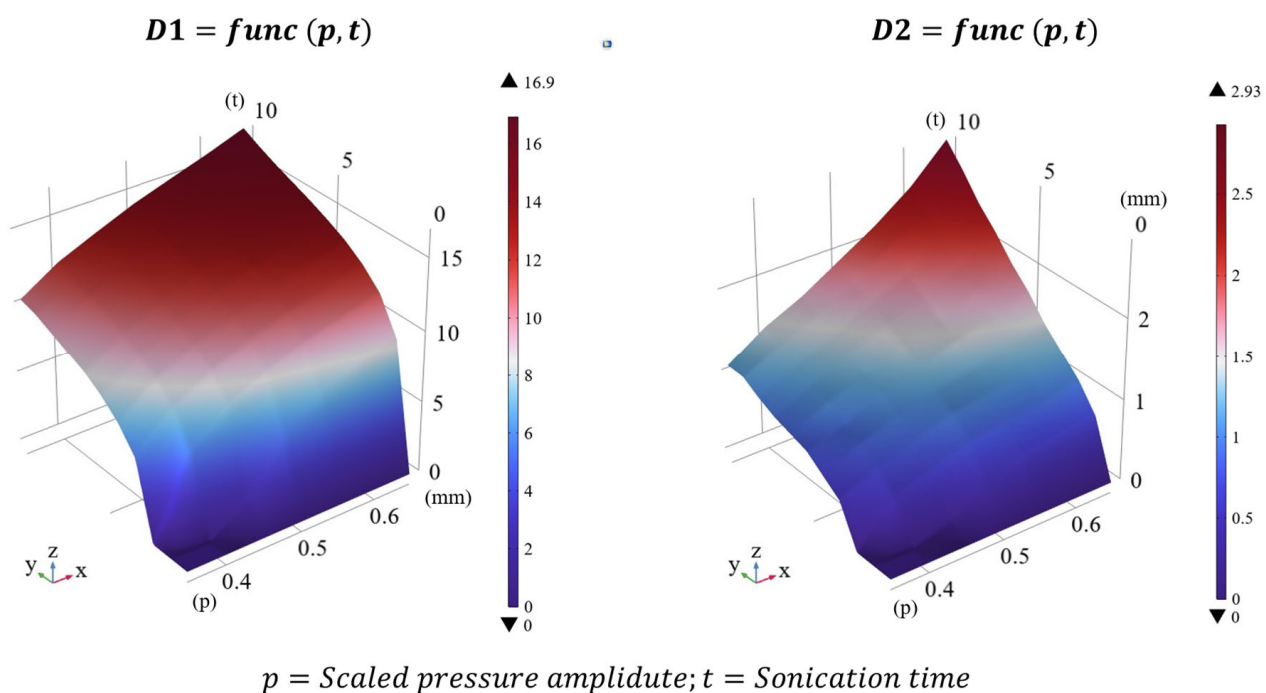


Figure 9. Polynomial function used as a surrogate of the COMSOL Multiphysics 6.2 model to estimate lesion dimensions based on a given combination of source pressure amplitude p (expressed through scale factors) and sonication time t .

Table 2. Analytical coefficients used to compute lesion dimensions with the polynomial function defined in Equation (1), as a function of source pressure amplitude and sonication time. The polynomial was derived from COMSOL Multiphysics 6.2 simulation data after optimization of the tissue absorption coefficient.

	a_0	a_1	a_2	a_3	a_4	a_5
D1	−19.7	0.2118	3.018	−0.0004684	$−3.731 \times 10^{-5}$	−0.1824
D2	−1.506	0.01441	0.1439	$−2.29 \times 10^{-5}$	0.00288	−0.02159

The second-order coefficients were considerably smaller than the first-order terms. This indicated that lesion growth with pressure and sonication time was primarily linear within the explored range, although nonlinear contributions were still captured by quadratic terms.

The percentage errors between lesion dimensions obtained from the COMSOL Multiphysics 6.2 simulation (considering $\alpha_{\text{tissueOptimized}} = 5.25$ [1/m]) and those predicted by the analytical polynomial results were below 3.39% for D1 and below 5.41% for D2. The polynomial function was therefore able to replicate the predictions of the COMSOL Multiphysics 6.2 model. To further verify this point, the errors between the polynomial function and the experimental data were calculated. As reported in Section 3.1.3, the mean errors between the COMSOL Multiphysics 6.2 predictions and the experimental data were 1.3 mm (10.7%) for D1 and 1.4 mm (26.8%) for D2. The mean errors between the function predictions and the experimental data—1.5 mm (11.8%) for D1 and 1.4 mm (27.3%) for D2—demonstrated that the proposed polynomial function could replace the COMSOL Multiphysics 6.2 simulation for fast or online predictions.

The MATLAB R2024b computation time was approximately 0.2 ms (measured on a system equipped with a 13th Gen Intel® Core™ i7-1370P processor 1.90 GHz), paving the way for potential real-time applications, including intraoperative re-planning in addition to the pre-operative planning traditionally associated with predictive models.

3.3. Polynomial Function Under Perfused Tissue Conditions

As expected, the inclusion of blood perfusion resulted in systematically smaller thermal lesions compared to the non-perfused case due to convective heat removal by blood flow.

It is worth noting that, in the present study, lesion size was defined through a threshold-based criterion ($T > 60$ °C, Section 3.1.3). Under single HIFU sonication conditions, the majority of the focal volume still exceeds this necrosis threshold even when perfusion is included. Therefore, moderate perfusion-induced variations in the temperature field do not translate into marked changes in the lesion extent. Based on these results, the shrinkage of lesion dimensions induced by perfusion was quantified, and the range of acoustic pressures required to produce thermally equivalent lesions with respect to the non-perfused case was identified.

Building on this analysis, the coefficients of the polynomial surrogate model—previously optimized using ex vivo chicken breast tissue for validation purposes—were recalculated to explicitly incorporate perfusion effects. This resulted in a corrected polynomial formulation that was more representative of perfused tissue conditions. For clinically relevant applications, the appropriate range of scale factors was identified between 0.36 (109.6 kPa) and 0.68 (207.13 kPa), compared to 0.35–0.65 for non-perfused ex vivo tissue, as shown in Figure 10. This range slightly extended beyond the upper limit experimentally associated with the thermally dominated regime under ex vivo conditions, a shift that can be reasonably attributed to perfusion-driven heat removal. The updated polynomial formulation is given by Equation (2), and the corresponding coefficients are reported in Table 3.

$$D_{1,2}(p, t) = \beta_0 + \beta_1 p + \beta_2 t + \beta_3 p^2 + \beta_4 t^2 + \beta_5 p t \quad (2)$$

Table 3. Analytical coefficients to compute lesion dimensions using the polynomial function in Equation (2) under perfused tissue conditions.

Perfused	β_0	β_1	β_2	β_3	β_4	β_5
D1	0.4855	0.01995	2.273	9.299×10^{-6}	0.008917	−0.2179
D2	−0.6157	0.003042	0.03537	1.449×10^{-5}	0.007565	−0.04404

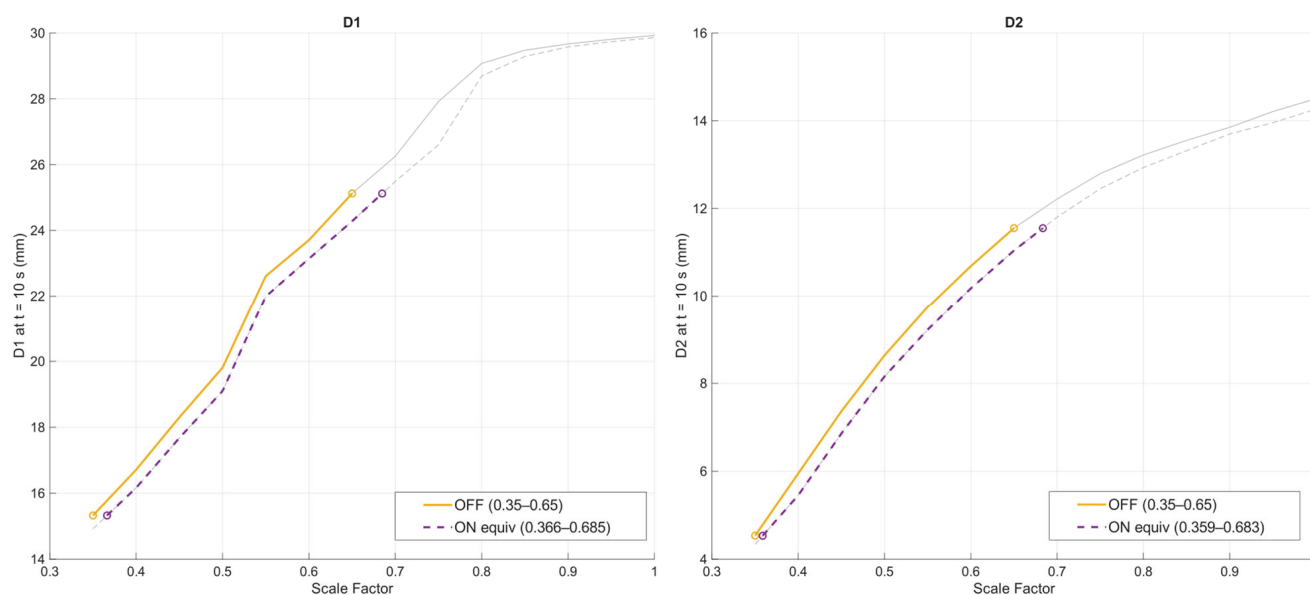


Figure 10. Comparison between non-perfused (OFF) and perfused (ON) conditions in terms of lesion size at the end of the sonication ($t = 10$ s). The yellow solid curves highlight the reference operating size at the end of the sonication ($t = 10$ s). The yellow solid curves highlight the reference operating window identified in the absence of blood perfusion (scale factor range 0.35–0.65), while the purple dashed curves indicate the equivalent operating window obtained when blood perfusion is enabled (scale factor range 0.36–0.68). Equivalence was defined by matching the final lesion dimensions produced in the non-perfused case.

3.4. Desktop Application for HIFU Thermal Treatment Planning

This inverse model-based application enables rapid and intuitive parameter selection without requiring computationally expensive numerical simulations, thus translating the polynomial model into a practical tool suitable for clinical workflows (Figure 11). The graphical user interface (GUI) allows the user to define the target lesion dimensions by specifying the desired values of D_1 and D_2 . Upon execution, the desktop application computes the corresponding shooting parameters, including source pressure amplitude, applied power percentage, and sonication time.

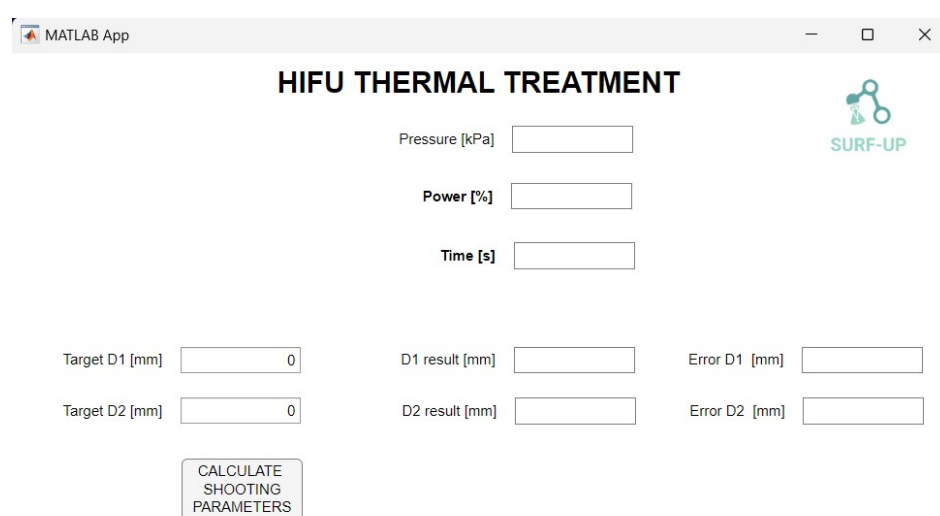


Figure 11. First version of the graphical user interface (GUI) of the desktop application for HIFU thermal treatment planning. The interface allows the user to specify the target lesion dimensions (D_1 and D_2) and computes the corresponding shooting parameters. The lesion dimensions predicted by the polynomial surrogate, together with the absolute deviations from the target values, are displayed to provide quantitative feedback on the planned treatment configuration.

In addition to the estimated shooting parameters, the interface displays the lesion dimensions computed by the polynomial model with the shooting parameters and absolute differences between these values and the target lesion dimensions specified by the user. This information provides quantitative feedback on the planned treatment configuration and supports the clinician in evaluating whether further adjustments or additional sonications should be considered to ensure adequate coverage of the target tumoral region.

The interface is designed to support an intuitive and streamlined workflow, allowing clinicians to iteratively adjust target lesion dimensions and rapidly obtain consistent treatment configurations within the validity range of the model.

4. Discussion and Conclusions

The objective of this study was to develop a predictive real-time method for the definition of lesion dimensions caused by thermal HIFU treatment.

A computational model was developed using COMSOL Multiphysics 6.2, simulating the relevant physical phenomena, including the propagation of acoustic waves and the resulting heat transfer due to the interaction of ultrasound with biological tissue. This mechanism leads to the conversion of acoustic energy into heat, enabling tissue ablation. The proposed computational model was then validated by comparing the COMSOL Multiphysics 6.2 lesion dimensions—by varying HIFU shooting parameter combinations, i.e., source pressure amplitude and sonication time—with the experimental outputs obtained under the same working conditions. Experimental tests were performed on ex vivo chicken breast tissue using a robotic UsgHIFU platform to enhance targeting accuracy. In this context, the model was formulated to account for heat transfer governed by thermal conduction only, consistent with the ex vivo validation conditions, where blood perfusion effects are inherently absent. The computational model error rate was 20% when compared to experimental results, which remains acceptable considering that margins up to 10 mm beyond the tumor edge are commonly regarded as safe in clinical practice. Together with mean error metrics, a Bland–Altman analysis was performed to assess the agreement between numerical predictions and experimental measurements, confirming stable error behavior and the absence of pathological bias across the investigated operating conditions.

Additionally, a detailed analysis of lesion morphology as a function of source pressure amplitude and sonication time showed that lesion size increased with both parameters, as expected. Given the experimental challenges in characterizing the thermal behavior of biological tissues and the shortage of thermal data in literature, a numerical optimization of the tissue absorption coefficient was carried out. This optimization was specific to the kind of tissue used in our experiments, i.e., ex vivo chicken breast. This led to improved results in lesion prediction compared to the non-optimized version. This method could be extended to other ex vivo tissues, such as the liver or pancreas, which are of particular interest in HIFU abdominal surgical applications.

Following simulation validation, an analytical polynomial function was derived to estimate lesion shape based on specific shooting parameters. This polynomial model could replace the physical simulation, achieving a maximum error of 5.41% in the calculation of lesion size compared to the COMSOL Multiphysics 6.2 prediction. The polynomial function required only 0.2 ms for lesion prediction definition, enabling potential real-time applications in clinical HIFU treatment planning, in contrast to full COMSOL Multiphysics 6.2 simulations, which typically require computation times on the order of hours.

After validation under ex vivo conditions, the framework was extended to include perfusion-driven heat exchange, introducing a numerical correction aimed at improving physiological relevance. This extension enabled the identification of an updated operating range and a corrected polynomial formulation for perfused tissue conditions.

Building upon this polynomial model, a desktop application based on the inverse use of the polynomial function was developed and integrated into the workflow. A simple and intuitive GUI allows clinicians to specify target lesion dimensions and computes the corresponding shooting parameters. By eliminating the need for computationally expensive numerical simulations, this application translates the polynomial model into a practical decision-support tool for clinical workflows. The proposed planning application demonstrates the feasibility of real-time, model-based treatment parameter selection and highlights the potential of this approach to support standardized HIFU treatments.

Future work will address the validation of the proposed framework on perfused organs and, where feasible, under in vivo experimental conditions, thereby advancing the framework toward clinical applicability. Moreover, further developments will focus on extending the discussed framework to additional tissue types and integrating the GUI with robotic path-planning algorithms, enabling automated trajectory control for sequential lesioning and complete volumetric ablation of the target region.

Author Contributions: Conceptualization, F.P., S.T., and A.M.; methodology, F.P., S.T., and A.M.; software, F.P.; formal analysis, F.P.; resources, S.T.; data curation, F.P.; writing—original draft preparation, F.P.; writing—review and editing, S.T. and A.M.; supervision, A.M.; funding acquisition, A.M. All authors have read and agreed to the published version of the manuscript.

Funding: This work was funded by “SURF-UP-Surgery by Using a Robotic Focused Ultrasound Platform” project under grant agreement no. FISA-2022-00770, within the Italiana FISA programme—Fondo Italiano Scienze Applicate—HEALTH sector.

Institutional Review Board Statement: Not applicable.

Informed Consent Statement: Not applicable.

Data Availability Statement: All relevant data supporting the conclusions of this article are included in the manuscript. The raw data will be made available by the authors on request.

Acknowledgments: Research activities were supported by the National Recovery and Resilience Plan (NRRP) funded by the European Union—NextGenerationEU—Project Title FUTURO—CUP J53D23006920006—Grant Assignment Decree No. 959 adopted on 30/06/2023 by the Italian Ministry of University and Research (MUR). The authors also thank the BRIEF “Biorobotics Research and Innovation Engineering Facilities” project (Project identification code IR0000036), funded by the National Recovery and Resilience Plan (NRRP), Mission 4 Component 2 Investment 3.1 of the Italian Ministry of University and Research, and co-funded by the European Union—NextGenerationEU, for sharing instrumentation. The authors would also like to acknowledge Franco Orsi from the Istituto Europeo di Oncologia (IEO, Milan, Italy) for his collaboration in understanding the clinical perspective related to HIFU technology. The authors also acknowledge Silvia Buratti for her contribution to the experimental activities.

Conflicts of Interest: The authors declare no conflicts of interest. The funders had no role in the design of the study; in the collection, analyses, or interpretation of data; in the writing of the manuscript; or in the decision to publish the results.

Abbreviations

The following abbreviations are used in this manuscript:

US	Ultrasound
HIFU	High-intensity focused ultrasound

USgHIFU	Ultrasound-guided high-intensity focused ultrasound
FEM	Finite element method
PML	Perfectly matched layer
dd-H ₂ O	Deionized and degassed water
GUI	Graphical user interface

References

- Haar, G.T. Therapeutic applications of ultrasound. *Prog. Biophys. Mol. Biol.* **2007**, *93*, 111–129. [CrossRef] [PubMed]
- Stratmeyer, M.E.; Christman, C.L. Biological effects of ultrasound. *Women Health* **1982**, *7*, 65–82. [CrossRef] [PubMed]
- Dewhurst, M.W.; Viglianti, B.L.; Lora-Michiels, M.; Hanson, M.; Hoopes, P.J. Basic principles of thermal dosimetry and thermal thresholds for tissue damage from hyperthermia. *Int. J. Hyperth.* **2003**, *19*, 267–294. [CrossRef] [PubMed]
- Haar, G.T. Ultrasound focal beam surgery. *Ultrasound Med. Biol.* **1995**, *21*, 1089–1100. [CrossRef]
- Fosse, E. Thermal ablation of benign and malignant tumours. *Minim. Invasive Ther. Allied Technol.* **2006**, *15*, 2–3. [CrossRef]
- Gunderman, A.; Montayre, R.; Ranjan, A.; Chen, Y. Review of Robot-Assisted HIFU Therapy. *Sensors* **2023**, *23*, 3707. [CrossRef]
- Mariani, A.; Morchi, L.; Diodato, A.; Tognarelli, S.; Menciassi, A. High-Intensity Focused Ultrasound Surgery Based on KUKA Robot: A Computer-Assisted Platform for Noninvasive Surgical Treatments on Static and Moving Organs. *IEEE Robot. Autom. Mag.* **2023**, *30*, 79–93. [CrossRef]
- Hill, C.R.; Haar, G.R.T. Review article: High intensity focused ultrasound—Potential for cancer treatment. *Br. J. Radiol.* **1995**, *68*, 1296–1303. [CrossRef]
- Ghasemifard, H.; Behnam, H.; Tavakkoli, J. High-Intensity Focused Ultrasound Lesion Detection Using Adaptive Compressive Sensing Based on Empirical Mode Decomposition. *J. Med. Signals Sens.* **2019**, *9*, 24. [CrossRef]
- Wu, J.; Nyborg, W.L. Ultrasound, cavitation bubbles and their interaction with cells. *Adv. Drug Deliv. Rev.* **2008**, *60*, 1103–1116. [CrossRef]
- Haar, G.T.; Coussios, C. High intensity focused ultrasound: Physical principles and devices. *Int. J. Hyperth.* **2007**, *23*, 89–104. [CrossRef] [PubMed]
- Haar, G.T. HIFU Tissue Ablation: Concept and Devices. *Adv. Exp. Med. Biol.* **2016**, *880*, 3–20. [CrossRef]
- Izadifar, Z.; Izadifar, Z.; Chapman, D.; Babyn, P. An Introduction to High Intensity Focused Ultrasound: Systematic Review on Principles, Devices, and Clinical Applications. *J. Clin. Med.* **2020**, *9*, 460. [CrossRef] [PubMed]
- Treeby, B.E.; Cox, B.T. k-Wave: MATLAB toolbox for the simulation and reconstruction of photoacoustic wave fields. *J. Biomed. Opt.* **2010**, *15*, 021314. [CrossRef] [PubMed]
- Rosnitskiy, P.B.; Khokhlova, T.D.; Schade, G.R.; Sapozhnikov, O.A.; Khokhlova, V.A. Treatment Planning and Aberration Correction Algorithm for HIFU Ablation of Renal Tumors. *IEEE Trans. Ultrason. Ferroelectr. Freq. Control* **2024**, *71*, 341–353. [CrossRef]
- Morelli, F.; Albanesi, A.; Ivanaj, A.; Buratti, S.; Parrotta, F.; Fu, J.; Tognarelli, S.; Menciassi, A.; De Momi, E.; Redaelli, A. High-Intensity Focused Ultrasound (HIFU) Modeling: In Vitro Validation and Integration into Patient-Specific Planning Tool. *Res. Sq.* **2025**. [CrossRef]
- Suomi, V.; Jaros, J.; Treeby, B.; Cleveland, R.O. Full modeling of high-intensity focused ultrasound and thermal heating in the kidney using realistic patient models. *IEEE Trans. Biomed. Eng.* **2018**, *65*, 969–979. [CrossRef]
- Cao, R.; Huang, Z.; Nabi, G.; Melzer, A. Patient-Specific 3-Dimensional Model for High-Intensity Focused Ultrasound Treatment Through the Rib Cage. *J. Ultrasound Med.* **2020**, *39*, 883–899. [CrossRef]
- Montienthong, P.; Rattanadecho, P. Focused ultrasound ablation for the treatment of patients with localized deformed breast cancer: Computer simulation. *J. Heat Transfer* **2019**, *141*, 101101. [CrossRef]
- Sanderson, S.G.; Easthope, B.; Farias, C.; Doddridge, I.; Cook, J.A.; Dahl, D.B.; Dillon, C.R. Characterizing Temperature-Dependent Acoustic and Thermal Tissue Properties for High-Intensity Focused Ultrasound Computational Modeling. *Int. J. Thermophys.* **2024**, *45*, 143. [CrossRef]
- Haar, G.T.; Rivens, I.; Wu, F. *Image-Guided Focused Ultrasound Therapy: Physics and Clinical Applications*; CRC Press: Boca Raton, FL, USA, 2024. Available online: <https://www.routledge.com/Image-guided-Focused-Ultrasound-Therapy-Physics-and-Clinical-Applications/Wu-Haar-Rivens/p/book/9781498711357> (accessed on 23 April 2025).
- High-Intensity Focused Ultrasound (HIFU) Propagation Through a Tissue Phantom. Available online: <https://www.comsol.com/model/high-intensity-focused-ultrasound-hifu-propagation-through-a-tissue-phantom-90191> (accessed on 23 April 2025).
- Diaz, M.A.; Solovchuk, M.A.; Sheu, T.W.H. A conservative numerical scheme for modeling nonlinear acoustic propagation in thermoviscous homogeneous media. *J. Comput. Phys.* **2018**, *363*, 200–230. [CrossRef]
- Erickson, R.R.; Zinn, B.T. Modeling of finite amplitude acoustic waves in closed cavities using the Galerkin method. *J. Acoust. Soc. Am.* **2003**, *113*, 1863–1870. [CrossRef]

25. Pennes, H.H. Analysis of tissue and arterial blood temperatures in the resting human forearm. *J. Appl. Physiol.* **1998**, *85*, 5–34. [[CrossRef](#)]
26. Tognarelli, S.; Ciuti, G.; Diodato, A.; Cafarelli, A.; Menciassi, A. Robotic Platform for High-Intensity Focused Ultrasound Surgery under Ultrasound Tracking: The FUTURA Platform. *J. Med. Robot. Res.* **2017**, *2*, 1740010. [[CrossRef](#)]
27. Van Beers, B.E.; Leconte, I.; Materne, R.; Smith, A.M.; Jamart, J.; Horsmans, Y. Hepatic Perfusion Parameters in Chronic Liver Disease: Dynamic CT Measurements Correlated with Disease Severity. *Am. J. Roentgenol.* **2001**, *176*, 667–673. [[CrossRef](#)]
28. Hayano, K.; Desai, G.S.; Kambadakone, A.R.; Fuentes, J.M.; Tanabe, K.K.; Sahani, D.V. Quantitative characterization of hepatocellular carcinoma and metastatic liver tumor by CT perfusion. *Cancer Imaging* **2013**, *13*, 512–519. [[CrossRef](#)]
29. Alabousi, M.; Ghai, S. Magnetic resonance imaging-guided ultrasound ablation for prostate cancer—A contemporary review of performance. *Front. Oncol.* **2023**, *12*, 1069518. [[CrossRef](#)]
30. Aslim, E.J.; Law, Y.X.T.; Fook-Chong, S.M.C.; Ho, H.S.S.; Yuen, J.S.P.; Lau, W.K.O.; Lee, L.S.; Cheng, C.W.S.; Ngo, N.T.; Law, Y.M.; et al. Defining prostate cancer size and treatment margin for focal therapy: Does intralesional heterogeneity impact the performance of multiparametric MRI? *BJU Int.* **2021**, *128*, 178–186. [[CrossRef](#)] [[PubMed](#)]

Disclaimer/Publisher’s Note: The statements, opinions and data contained in all publications are solely those of the individual author(s) and contributor(s) and not of MDPI and/or the editor(s). MDPI and/or the editor(s) disclaim responsibility for any injury to people or property resulting from any ideas, methods, instructions or products referred to in the content.